DALTON
FULL PAPER

Electronic structures of copper(II) complexes of tetradentate hydroquinone-containing Schiff bases †

Elizabeth H. Charles,[a] Li Mei Lindy Chia,[a] Joanne Rothery,[a] Emma L. Watson,[a] Eric J. L. McInnes,[b] Robert D. Farley,[c] Adam J. Bridgeman,[a] Frank E. Mabbs,[b] Christopher C. Rowlands[c] and Malcolm A. Halcrow*[d]

[a] *Department of Chemistry, University of Cambridge, Lensfield Road, Cambridge, UK CB2 1EW*
[b] *EPSRC CW EPR Service Centre, Department of Chemistry, University of Manchester, Oxford Road, Manchester, UK M13 9PL*
[c] *EPSRC ENDOR Service Centre, Department of Chemistry, University of Wales at Cardiff, PO Box 912, Cardiff, UK CF1 3TB*
[d] *School of Chemistry, University of Leeds, Woodhouse Lane, Leeds, UK LS2 9JT. E-mail: M.A.Halcrow@chem.leeds.ac.uk*

Received 23rd March 1999, Accepted 23rd April 1999

Reaction of 2,5-dihydroxybenzaldehyde with 0.5 equivalent of 1,2-diaminoethane, *trans*-1,2-diaminocyclohexane or 1,2-diaminobenzene in the absence or presence of hydrated $Cu(O_2CMe)_2 \cdot H_2O$ in refluxing MeOH respectively afforded the ligands H_2L and complexes [Cu(L)] [H_2L = *N*,*N*′-bis(2,5-dihydroxybenzylidene)-1,2-diaminoethane (H_2L^1), *N*,*N*′-bis(2,5-dihydroxybenzylidene)-*trans*-1,2-diaminocyclohexane (H_2L^2), *N*,*N*′-bis(2,5-dihydroxybenzylidene)-1,2-diaminobenzene (H_2L^3)] in yields of 66–86%. Using X- and Q-band EPR and ^{1}H and ^{14}N X-band ENDOR data, the following fractional unpaired spin densities were calculated: $\rho\{Cu\} = 0.75$, $\rho\{N\} = 0.07$, $\rho\{O\} \leq 0.04$, $\rho\{H\} = 0.01$. Density functional (DF), intermediate neglect of differential overlap with spectroscopic parameterisation (INDO/S) and extended Hückel calculations of [Cu(MeOsalen)] broadly reproduced these results, the DF calculations demonstrating that the phenoxide oxygen lone pair is misdirected away from the Cu–O bond. The cyclic voltammograms of the ligands and complexes in dmf–0.1 M $NBu^n_4PF_6$ at 293 K showed a single oxidation of the two ligand hydroquinone groups, and two principal daughter processes: an irreversible reduction of the initial oxidised quinone, probably in a monoprotonated or metallated form; and a more cathodic reduction and associated reoxidation indicative of a proton- and metal ion-induced electrochemical step–chemical step–electrochemical step reaction.

Introduction

The redox, spectroscopic, structural and photochemistries of catecholate and *ortho*-semiquinone complexes continue to be very well studied.[1] However, a much smaller literature exists for metal complexes of ligands containing σ-co-ordinated *para*-hydroquinone or *para*-benzoquinone groups,[2–12] despite the potential for novel redox chemistry in such compounds. Indeed, we are aware of only three electrochemical studies of *para*-hydroquinonate complexes, one of which appeared during the course of this work.[4,5,12] We note that H_2L^1, H_2L^2 and a small number of their complexes have been briefly described, although in all cases only basic analytical data (IR, CHN) were reported.[7] Since H_2L^1 can be thought of as a "non-innocent" analogue of the classic Schiff base ligand H_2salen, we were interested to examine in more detail the co-ordination chemistry of hydroquinone-containing Schiff ligands of this type. We report here the syntheses, and a preliminary voltammetric study, of the copper(II) complexes of H_2L^1–H_2L^3. Also described is a comprehensive EPR, ENDOR and theoretical characterisation of these complexes, which has allowed us to define in some detail the spin distribution within this ubiquitous class of compounds.

† Abbreviations used: 2,5-dhb = 2,5-dihydroxybenzaldehyde; H_2MeOsalen = *N*,*N*′-bis(5-methoxysalicylidene)-1,2-diaminoethane; H_2MeOsalophen = *N*,*N*′-bis(5-methoxysalicylidene)-1,2-diaminobenzene; H_2salophen = *N*,*N*′-bis(salicylidene)-1,2-diaminobenzene.

Results and discussion

Syntheses and characterisation of the Schiff base ligands and complexes

Following the usual method for the synthesis of H_2salen and its analogues,[13] treatment of 2,5-dhb with 0.5 molar equivalent of the appropriate diamine in refluxing MeOH for 3 h afforded H_2L^1, H_2L^2 or H_2L^3 as analytically pure solids in 72–86% yield. The ^{1}H NMR spectra of H_2L^1–H_2L^3 in $(CD_3)_2SO$ are consistent with the proposed molecular structures, showing resonances for the 2- and 5-hydroxyl groups close to δ 12.5 and 9.0, respectively, and for the aldimine proton at δ 8.4–8.8, in addition to the appropriate pattern of aryl and alkyl resonances. In keeping with the microanalysis of H_2L^3, one mole equivalent of MeOH is also revealed in the ^{1}H spectrum of this compound. Attempted syntheses of H_2L^3 in $CHCl_3$ or MeCN, intended to give solvent-free ligand, afforded mixtures of products that we were unable to separate. The monoimine HL[4] was also prepared as a model compound for the electrochemical studies, being obtained in analytical purity by reaction of 2,5-dhb with $MeNH_2$ in MeOH.

The complexes [Cu(L)] (L^{2-} = $[L^1]^{2-}$, $[L^2]^{2-}$ or $[L^3]^{2-}$) were synthesized under the same conditions employed for the "free" ligands, with the addition of 0.5 molar equivalent of $Cu(O_2CMe)_2 \cdot H_2O$ as template ion. These reactions proceeded cleanly, affording brown precipitates, which were filtered off, washed with MeOH and Et_2O and dried *in vacuo*. Microanalysis was consistent with the formulation of these solids as

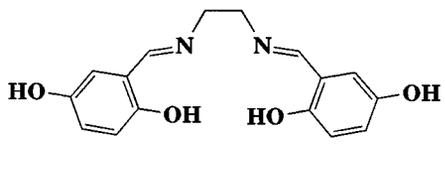

H_2L^1

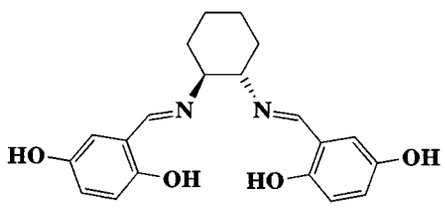

H_2L^2

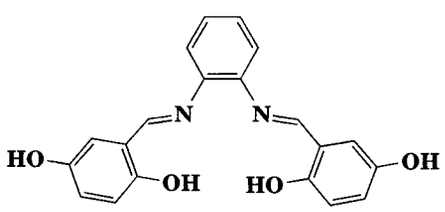

H_2L^3

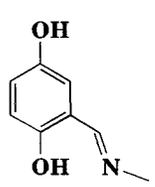

HL^4

the desired compounds as hydrates or methanol solvates, while FAB mass spectrometry confirmed the presence of the intact complex molecule while showing no significant fragmentation or impurity peaks. As for the "free" ligands, attempted template syntheses in $CHCl_3$ or MeCN did not yield pure products. However, mixing of MeCN solutions of $Cu(O_2CMe)_2{\cdot}H_2O$ and preformed H_2L^2 or H_2L^3 resulted in the precipitation of brown microcrystals, both of which reproducibly analysed for $[Cu(L)]{\cdot}0.5H_2O{\cdot}0.5MeCN$ ($L^{2-} = [L^2]^{2-}$ or $[L^3]^{2-}$).

The ligands H_2L^2 and H_2L^3 are sparingly soluble in MeCN and $MeNO_2$. However, H_2L^1 and the complexes are insoluble in all common solvents except dmf, dma (dimethylacetamide) and dmso, in which they have only sparing solubilities. This low solubility has severely hampered our efforts to recrystallise these complexes, and we have thus far been unable to obtain X-ray quality crystals of any of the compounds in this study.

The UV/visible spectra of $[Cu(L^1)]$ and $[Cu(L^2)]$ in dmf at 298 K are barely distinguishable, these two complexes showing a d–d maximum close to ν_{max} 17500 cm^{-1} with $\varepsilon_{max} = 420$–430 $M^{-1}\,cm^{-1}$. This band is at the high end of the range of energies reported for other copper(II) complexes of salen-type ligands, which lie between ν_{max} 15200 and 17900 cm^{-1}.[14–19] For $[Cu(L^3)]$ this peak is obscured by more intense ligand-derived absorptions, occurring as a shoulder close to $\nu_{max} = 15400\ cm^{-1}$. The remaining bands in all the complexes can be assigned to $\pi \longrightarrow \pi^*$ transitions within the co-ordinated Schiff bases.[14,20] These $\pi \longrightarrow \pi^*$ absorptions lie up to 5000 cm^{-1} lower in energy than those previously reported for copper(II) complexes of salen and salophen,[14,16,18,20–22] consistent with the increased electron-richness of the dihydroxyphenyl rings in $[L^1]^{2-}$–$[L^3]^{2-}$.

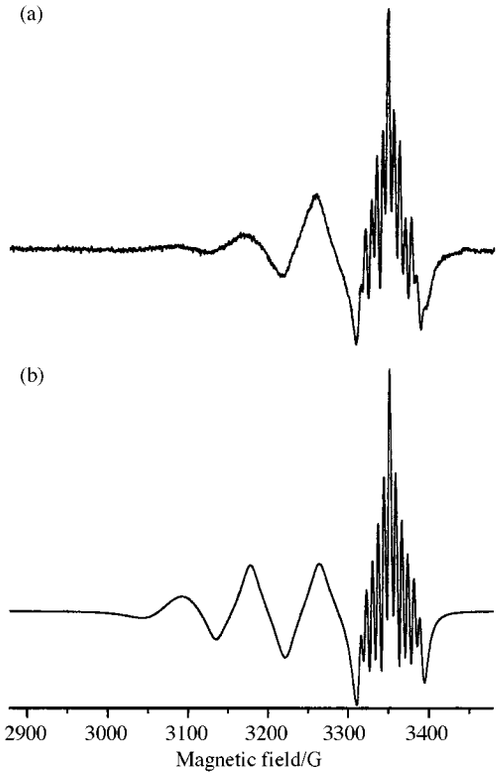

Fig. 1 Second-derivative EPR spectrum of $[Cu(L^3)]$ in 10:1 dmf:toluene solution at 298 K: (a) experimental X-band spectrum ($\nu = 9.445$ GHz); (b) simulation using $\langle g \rangle = 2.100$, $\langle A\{^{63,65}Cu\} \rangle = 85.2 \times 10^{-4}$, $\langle A\{^{14}N\} \rangle = 13.7 \times 10^{-4}$, $\langle A\{^{1}H\} \rangle = 7.4 \times 10^{-4}$ cm^{-1} and linewidth coefficients $A = 19$, $B = 15$ and $C = 5$ G for the expression $\Delta B = A + Bm_I + Cm_I^2$, where ΔB is the peak-to-peak linewidth of the individual copper hyperfine lines.

EPR and ENDOR spectroscopy of [Cu(L)] ($L^{2-} = [L^1]^{2-}$–$[L^3]^{2-}$)

The X-band EPR spectra of [Cu(L)] ($L^{2-} = [L^1]^{2-}$–$[L^3]^{2-}$) in 10:1 dmf:toluene solution at 293 K are essentially identical, the isotropic EPR parameters derived from them closely matching those reported previously for other copper(II) complexes of bis-salicylaldimine ligands.[19,21–25] The spectra consist of the expected 4-line pattern from coupling to $^{63,65}Cu$ ($I = \frac{3}{2}$), with $\langle g \rangle = 2.100$ ($L^{2-} = [L^1]^{2-}$), 2.096 ($L^{2-} = [L^2]^{2-}$) and 2.097 {$L^{2-} = [L^3]^{2-}$; Fig. 1(a)}. Although suffering from m_I-dependent line broadening, the $m_I = -\frac{3}{2}$ line in each spectrum shows superhyperfine coupling to two ^{14}N and two ^{1}H nuclei, which correspond to the ligand aldimino N=CH protons.[26] The spectra for all three complexes were simulated assuming $\langle A\{^{63,65}Cu\} \rangle = 85.2 \times 10^{-4}$, $\langle A\{^{14}N\} \rangle = 13.7 \times 10^{-4}$ and $\langle A\{^{1}H\} \rangle = 7.4 \times 10^{-4}$ cm^{-1} with errors of $\pm 0.5 \times 10^{-4}$ cm^{-1} [Fig. 1(b)].

In frozen dmf:toluene solution the X-band EPR spectra exhibit the axial pattern typical of tetragonal copper(II) complexes with an approximate $\{d_{xy}\}^1$ or $\{d_{x^2-y^2}\}^1$ ground state,[27] showing $g_\parallel \approx 2.21$, $g_\perp \approx 2.05$, $A_\parallel\{^{63,65}Cu\} \approx 200 \times 10^{-4}$ cm^{-1} [Fig. 2(a)]. Interestingly, the perpendicular regions of these spectra show clearly resolved hyperfine and superhyperfine interactions. The axial symmetry of the system was confirmed by obtaining spectra at Q band, which reproduced the g values derived from X-band data well but no longer showed resolved coupling in the perpendicular region [Fig. 2(c)]. No spin-triplet signal suggesting partial dimerisation of the complexes in solution[25] was detected.

Given the unusually well resolved anisotropic X-band spectra shown by these copper(II) complexes, $[Cu(L^1)]$ and $[Cu(L^3)]$ were further investigated by X-band ENDOR spectroscopy; no study of $[Cu(L^2)]$ was attempted because of its lower solubility. All ENDOR measurements were performed in frozen dmf:toluene solution at 10 K; ^{1}H and ^{14}N spectra at 8 ($[Cu(L^1)]$) and 10

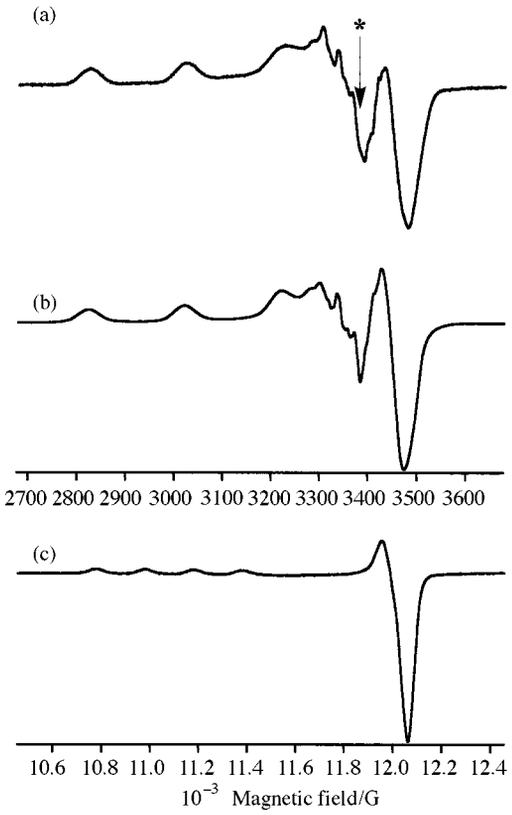

Fig. 2 First derivative EPR spectra of [Cu(L^3)] in 10:1 dmf:toluene solution at 120 K: (a) experimental X-band spectrum (ν = 9.445 GHz); (b) simulated X, using fitting parameters described in the text; (c) experimental Q-band spectrum (ν = 34.200 GHz). The * shows the field position for the ENDOR spectrum shown in Fig. 3.

([Cu(L^3)]) different applied fields were measured, covering the complete EPR absorption for the two compounds. In the following discussion it is assumed that the molecular, g and $A\{^{63,65}\text{Cu}\}$ axes in the ENDOR and EPR experiments are coincident, with the parallel direction corresponding to the molecular z axis [Scheme 1(a)]. The local ^{14}N tensor is assumed to be axial, with $A_\parallel\{^{14}\text{N}\}$ aligned along the corresponding Cu–N bond [Scheme 1(b)].

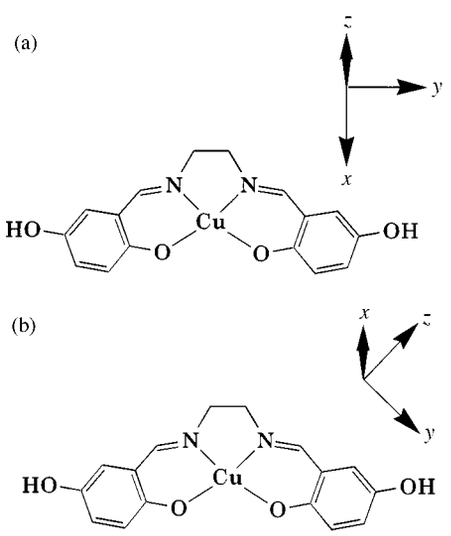

Scheme 1 Molecular axes for copper(II) complexes of salen-type ligands with C_{2v} symmetry: (a) true molecular axes, and axes for the g and $A\{^{63,65}\text{Cu}\}$ tensors; (b) local axes for the $A\{^{14}\text{N}\}$ tensor.

Both compounds gave single crystal-type ^{14}N ENDOR spectra at a field corresponding to the lowest-field $A_\parallel\{^{63,65}\text{Cu}\}$ hyperfine transition, exhibiting well resolved $A_\perp\{^{14}\text{N}\}$ couplings.

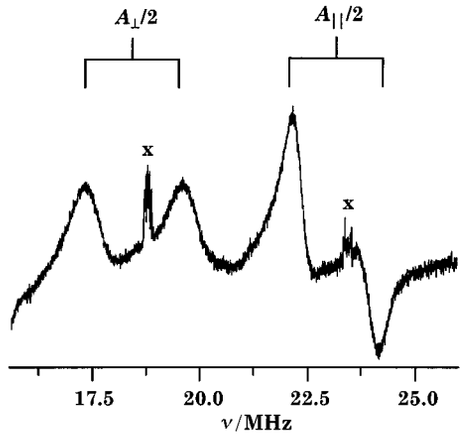

Fig. 3 X-Band ^{14}N ($2\nu_N$ = 2.04 MHz) ENDOR spectrum of [Cu(L^3)] in 10:1 dmf:toluene solution at 10 K. The field position is marked on Fig. 2. Features 'x' are radiofrequency artifacts.

At higher fields both $A_\parallel\{^{14}\text{N}\}$ and $A_\perp\{^{14}\text{N}\}$ features were observed (Fig. 3), since the $m_I = -\frac{3}{2}$ $A_\parallel\{^{63,65}\text{Cu}\}$ feature overlays the EPR $g_\perp$ region. Importantly both these couplings were essentially invariant at different applied fields across the perpendicular region of the spectrum, showing that the spectra had true powder character reflecting the selection of the vast majority of molecular orientations within the EPR linewidth. The following coupling constants were derived: for [Cu(L^1)], $|A_\parallel\{^{14}\text{N}\}| = 46.5$ (14.3×10^{-4}) and $|A_\perp\{^{14}\text{N}\}| = 38.9$ MHz $(13.0 \times 10^{-4}$ cm$^{-1})$; for [Cu(L^3)], $|A_\parallel\{^{14}\text{N}\}| = 46.3$ (14.3×10^{-4}) and $|A_\perp\{^{14}\text{N}\}| = 36.9$ MHz $(12.3 \times 10^{-4}$ cm$^{-1})$. These must correspond to the true values, given the relative alignments of the axes for the $A\{^{14}\text{N}\}$ and $A\{^{63,65}\text{Cu}\}$ tensors (Scheme 1).[28] All the ^{14}N ENDOR spectra were significantly broadened, presumably by unresolved quadrupolar couplings, which prevented the detection of second-order splittings that might be expected at these frequencies.

The ^{1}H ENDOR spectra obtained at the same field employed for the ^{14}N parallel spectra (Fig. 2) were also well resolved. For [Cu(L^1)] 5 of the 6 expected proton environments were detected, with $|A\{^1\text{H}\}| = 4.5$, 2.3, 1.7, 0.7 and 0.2 MHz (1.5, 0.7, 0.5, 0.2 and 0.1×10^{-4} cm^{-1}); we assign the strongest of these couplings to the alkyl CH_2 protons of the [L^1]$^-$ ligand, and the other values to the C–H and O–H environments of the hydroquinonate rings. For [Cu(L^3)], 4 distinct proton coupling constants were observed at $|A\{^1\text{H}\}| = 1.7$, 1.3, 0.7 and 0.3 MHz (0.5, 0.4, 0.2 and 0.1×10^{-4} cm^{-1}). A weak low frequency feature corresponding to $|A\{^1\text{H}\}| = 17.5$ and 15.6 MHz for [Cu(L^1)] and [Cu(L^3)], respectively, *might* arise from one peak of the aldimine proton resonance; however, the putative high frequency component of this doublet is obscured by the stronger ^{14}N peaks, preventing corroboration of this assignment. Unfortunately, at higher fields extremely complex powder-type ^{1}H spectra were obtained, which could not be unambiguously interpreted. The orientations and symmetries of the local axes for these protons are therefore unknown, and no more detailed analysis is possible.

The frozen solution X-band EPR spectra of [Cu(L^1)] and [Cu(L^3)] were simulated using the ENDOR results for $A\{^{14}\text{N}\}$. In the absence of conclusive ^{1}H ENDOR data, the superhyperfine interaction to the aldimine N=C*H* nuclei was treated as isotropic, the simulations proving sensitive to the value of this coupling. Good simulations were obtained for both [Cu(L^1)] and [Cu(L^3)] using the following parameters [Fig. 2(b)], which differ only in the linewidths employed for the two complexes: $g_\parallel = 2.210$, $g_\perp = 2.045$, $A_\parallel\{^{63,65}\text{Cu}\} = 203 \times 10^{-4}$, $A_\perp\{^{63,65}\text{Cu}\} = 27 \times 10^{-4}$, $A_\parallel\{^{14}\text{N}\} = 12 \times 10^{-4}$, $A_\perp\{^{14}\text{N}\} = 15 \times 10^{-4}$, $A_\parallel\{^1\text{H}\} = A_\perp\{^1\text{H}\} = 7 \times 10^{-4}$ cm^{-1} $W_\parallel = 15$, $W_\perp = 14$ ([Cu(L^1)]) or 10 G ([Cu(L^3)]). Note that these EPR simulations fit all the g and tensors to the true molecular axes [Scheme 1(a)], so that

$A_{\parallel}\{^{14}N\}$ from the EPR simulations is equivalent to the true $A_{\perp}\{^{14}N\}$ value measured by ENDOR.

EPR Calculations

The spin-Hamiltonian parameters from the EPR study were employed to calculate covalency parameters according to the ligand-field method of Kivelson and Neiman.[29,30] Unfortunately, the original description of this approach[29] contains several misprinted equations and constants, which do not seem to have been corrected in later reports. We will therefore discuss our calculations in detail.

Metal–ligand bonding about a D_{4h} copper(II) centre is described according to eqns. (1)–(4): where λ_0 is the spin–orbit

$$g_{\parallel} - g_e = -8\rho\{\alpha\beta - \alpha'\beta S - [\alpha'(1 - \beta^2)^{\frac{1}{2}}T(n)/2]\} \quad (1)$$

$$g_{\perp} - g_e = -2\mu\{\alpha\beta - \alpha'\delta S - [\alpha'(1 - \delta^2)^{\frac{1}{2}}T(n)/2^{\frac{1}{2}}]\} \quad (2)$$

$$A_{\parallel}\{^{63,65}Cu\} = P\left[-\frac{4}{7}\alpha^2 - \kappa_0 + (g_{\parallel} - g_e) + \frac{3}{7}(g_{\perp} - g_e) - 8\rho\{\alpha'\beta S + [\alpha'(1 - \beta^2)^{\frac{1}{2}}T(n)/2]\} - \frac{6}{7}\mu\{\alpha'\delta S + [\alpha'(1 - \delta^2)^{\frac{1}{2}}T(n)/2^{\frac{1}{2}}]\}\right] \quad (3)$$

$$A_{\perp}\{^{63,65}Cu\} = P\left[\frac{2}{7}\alpha^2 - \kappa_0 + \frac{1}{4}(g_{\perp} - g_e) - \mu\{\alpha'\delta S + [\alpha'(1 - \delta^2)^{\frac{1}{2}}T(n)/2^{\frac{1}{2}}]\}\right] \quad (4)$$

coupling constant for the free copper(II) ion (-828 cm^{-1} [31]), κ_0 is the Fermi contact constant for the free ion (0.33 [26,29,31]), S is the Cu–N/O overlap integral (0.093 for N, 0.076 for O) assuming Cu–N/O bonds of 1.9 Å,[26,29] the constant $T(n)$ has the value 0.333 for nitrogen ligation and 0.220 for O, the constant P has the value 0.036 cm^{-1} [31] and μ and ρ have the definitions[29] in eqns. (5) and (6). Here, α^2 and α'^2 correspond respectively to

$$\rho = \lambda_0\alpha\beta/\Delta E_{x^2-y^2} \quad (5)$$

$$\mu = \lambda_0\alpha\delta/\Delta E_{xz} \quad (6)$$

covalency factors at Cu$\{d_{xy}\}$ and the ligand donor atoms for metal–ligand σ bonding, which by normalisation must obey eqn. (7). Similarly, β and δ are covalency factors at Cu for

$$\alpha^2 + \alpha'^2 - 2\alpha\alpha' S = 1 \quad (7)$$

in-plane metal–ligand π bonding (Cu$\{d_{x^2-y^2}\}$) and out-of-plane π bonding (Cu$\{d_{xz}/d_{yz}\}$), respectively. Although these equations do not allow for d-orbital mixing, which is possible in the C_{2v} point group exhibited by [Cu(L^1)] and [Cu(L^3)] (Scheme 1), the axial symmetry of the g and A tensors for our compounds suggests that this approximation is justified. Several calculations of this type for [Cu(salen)] and related Schiff base complexes have been reported previously,[21,24,26,29,30] with somewhat contradictory results which reflect different values of $\Delta E_{x^2-y^2}$, ΔE_{xz}, S and $T(n)$, and/or an incorrect value of κ_0, used by each group.

We employed average values of $S = 0.085$ and $T(n) = 0.276$ in eqns. (1)–(4), to reflect the N_2O_2 ligation at Cu. The d–d transition energies are more problematic, however, particularly since no single crystal UV/vis data are available for [Cu(salophen)]. For [Cu(salen)], the $\Delta E_{x^2-y^2}$ energy has been shown to lie close to the d–d maximum.[14,32–34] Therefore, we estimated $\Delta E_{x^2-y^2} = 17500$ cm^{-1} for [Cu(L^1)] and 16000 cm^{-1} for [Cu(L^3)] (from the UV/vis of [Cu(MeOsalophen)], which shows a maximum here in dmf[21]). The ΔE_{xz} transition has not been unambiguously assigned for [Cu(salen)], and may be obscured by $\Delta E_{x^2-y^2}$ or by charge transfer bands with $\nu_{max} \leq 22000$ cm^{-1}.[14,34] We therefore performed calculations using ΔE_{xz} values corresponding to both of the possible ranges (21000–25000 cm^{-1} for [Cu(salen)] [14,32–34]), and assuming that the ratio $\Delta E_{x^2-y^2} : \Delta E_{xz}$ is the same for [Cu(L^1)] and [Cu(L^3)] (Table 1).

Table 1 Covalency factors for [Cu(L^1)] and [Cu(L^3)] calculated from eqns. (1)–(7), showing the estimated d–d transition energies employed in the calculations

	[Cu(L^1)]		[Cu(L^3)]	
$\Delta E_{x^2-y^2}$/cm^{-1}	17500	17500	16000	16000
ΔE_{xz}/cm^{-1}	21000	25000	19000	23000
α^2	0.84	0.83	0.84	0.83
α'^2	0.24	0.25	0.24	0.25
β^2	0.72	0.72	0.68	0.68
δ^2	0.73	0.86	0.67	0.79

The covalency factors were derived from eqns. (1)–(4) by an iterative procedure.[29] The results of these calculations, together with the estimated transition energies employed, are listed in Table 1. Of our calculated parameters, only β^2 and δ^2 are sensitive to the values of the estimated d–d transition energies. Our values for α^2 are close to values previously calculated by others for [Cu(salen)] from less complete EPR data,[21,24,30] while our values of β^2 are similar to those recently derived by Srinivas and co-workers.[21,24] Our values of δ^2 seem anomalously low in the light of our MO calculations which imply negligible out-of-plane π bonding (see below); this suggests that we may have significantly underestimated ΔE_{xz} for the two compounds. Nonetheless, the insensitivity of α^2 to $\Delta E_{x^2-y^2}$ and ΔE_{xz} implies that, despite the lack of accurate transition energies, we have a consistent description of the metal–ligand σ bonding in these complexes.

The α'^2 parameters calculated above correspond to a cumulative value for the 2 N- and 2 O-donor atoms of the chelate ligands.[35] A value $\alpha'^2\{N\}$ for the 2 N-donors only can be derived from $A\{^{14}N\}$, using eqns. (8) and (9) which assume coupling to 2 sp^2-hybridised N atoms;[26] ‡ where γ_L is the magnetogyric ratio of the ^{14}N nucleus (0.404), $\delta(\boldsymbol{r})$ is the value of the 2s function at the nitrogen nucleus (33.4×10^{24}) and $\langle r^{-3}\rangle_p$ for nitrogen 2p orbitals has the value 21.1×10^{24}.[29] Using this method we obtain $\alpha'^2\{N\} = 0.16$ (*i.e.* 0.08 per N atom) for both complexes. We can also derive a covalency factor for the ligand hydrogen nuclei, by dividing $\Sigma\langle A\{^1H\}\rangle$ by the hyperfine constant of the free H atom (1420.4 MHz).[36] Assuming $\langle A\{^1H\}\rangle \approx A_{\parallel}\{^1H\}$, this equates to a total $\alpha'^2\{H\} = 0.04$, of which *ca.* 80% derives from the aldimine group protons. Finally, using eqn. (10), which assumes zero overlap between non-bonded atoms, we obtain $\alpha'^2\{O\} \leq 0.08$. This represents an upper limit for $\alpha'^2\{O\}$ since eqn. (10) does not allow for delocalisation of the unpaired spin onto the ligand C nuclei ($\alpha'^2\{C\}$), which should be of a similar magnitude to $\alpha'^2\{H\}$. Nonetheless, it is apparent that for [Cu(L^1)] and [Cu(L^3)] greater σ covalency exists within the copper–ligand bonds to the 'softer' sp^2 N-donors compared to the 'harder' anionic O-donors. There is good agreement between values of α'^2 calculated from eqns. (1)–(5) (0.31) and $\alpha'^2\{N\} + \alpha'^2\{H\} + \alpha'^2\{O\}$ from eqns. (8)–(10) (0.28).

$$A_{\parallel}\{^{14}N\} = \left(\frac{\alpha'\{^{14}N\}^2}{2}\right)(2\gamma_L\beta_O\beta_N)\left[-\frac{8\pi}{9}\delta(\boldsymbol{r}) + \frac{8}{15}\langle r^{-3}\rangle_p\right] \quad (8)$$

$$A_{\perp}\{^{14}N\} = \left(\frac{\alpha'\{^{14}N\}^2}{2}\right)(2\gamma_L\beta_O\beta_N)\left[-\frac{8\pi}{9}\delta(\boldsymbol{r}) - \frac{1}{15}\langle r^{-3}\rangle_p\right] \quad (9)$$

‡ Earlier EPR calculations of copper(II) salicylaldimine complexes in refs. 24, 29 and 30 did not correct eqns. (8) and (9) to describe coupling to 2 rather than 4 equivalent ligand donors. Values of α'^2 calculated from $A\{^{14}N\}$ in these references are therefore misleading.

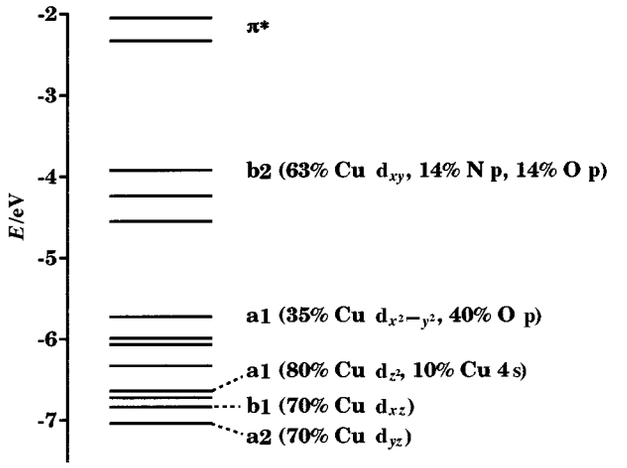

Fig. 4 Kohn–Sham eigenvalue diagram for the $^2B_2$ ground state of [Cu(MeOsalen)], as calculated by the DF method (1 eV ≈ 8065.5 cm^{-1}). The percentage character of the metal-dominated functions is given with symmetry labels corresponding to the approximate C_{2v} symmetry of the first co-ordination sphere. The unlabelled functions are all ligand-based π orbitals with varying amounts of metal d$_{xz}$ and d$_{yz}$ contributions.

$$\alpha^2 + \alpha'^2\{N\} + \alpha'^2\{O\} + \alpha'^2\{H\} - 2\alpha\alpha'\{N\}S\{Cu,N\} - 2\alpha\alpha'\{O\}S\{Cu,O\} = 1 \quad (10)$$

MO Calculations of [Cu(MeOsalen)]

For comparison with our EPR results, calculations were carried out using crystal structure coordinates for [Cu(MeOsalen)][24] at the Extended Hückel (EH), Intermediate Neglect of Differential Overlap with Spectroscopic parameterisation (INDO/S) and Density Functional (DF) levels. The three methods gave similar descriptions of bonding within the complex, with only slight variations in the orbital ordering. Since the DF calculation is likely to afford the most accurate description of the molecule only this will be discussed in detail.

Fig. 4 shows the eigenvalues and approximate descriptions of the highest lying orbitals in the complex from the DF study. The calculations predict a $^2B_2$ ground state in the approximate C_{2v} symmetry of the copper ion, with a singly occupied orbital (SOMO) of mainly d$_{xy}$ character. The low energy of the copper d$_{xz}$ and d$_{yz}$ orbitals suggests that the out-of-plane π interaction is small. This is confirmed by the very small changes in the Mulliken populations for these two orbitals compared to their values in a purely ionic crystal field. The low energy of the copper d$_{z^2}$ orbital is mainly a result of s–d hybridisation.[37] The copper d$_{x^2-y^2}$ orbital suffers a large ligand-field effect, predominantly due to interaction with the in-plane lone pairs of the co-ordinated oxygen atoms. Analysis of the density matrix leads to Cu–N and Cu–O bond orders of 0.68 and 0.57 respectively, reflecting the poor donor ability of the more electronegative oxygen and the antibonding role of its lone pairs. Interestingly, the DF calculation shows that the O(1) lone pair is misdirected away from the Cu–O vector (Fig. 5), as previously proposed for [Co(salen)].[38] This feature is not reproduced by the EH or INDO/S calculations, which show the O(1) lone pair aligned along the Cu–O bond.

In order to compare the results of the EPR and MO calculations the EPR-derived covalency factors must be converted into fractional spin densities according to eqns. (11) and (12) (E = N, O or H). The resultant experimental composition of the

$$\rho\{Cu\} = \frac{\alpha^2}{[\alpha^2 + \alpha'^2\{N\} + \alpha'^2\{O\} + \alpha'^2\{H\}]} \quad (11)$$

$$\rho\{E\} = \frac{\alpha'^2\{E\}}{2[\alpha^2 + \alpha'^2\{N\} + \alpha'^2\{O\} + \alpha'^2\{H\}]} \quad (12)$$

Table 2 Experimental fractional unpaired spin densities for [Cu(L^1)], and calculated fractional spin densities for the SOMO of [Cu(MeO-salen)]. The atom numbering scheme is shown in Fig. 5

	Experimental	EH	INDO/S	DF
ρ{Cu}	0.75	0.44	0.52	0.63
ρ{N}	0.07	0.16	0.10	0.07
ρ{O(1)}	≤0.04	0.07	0.09	0.07
ρ{H(7)}	0.01	0.01	0.01	0.01
$\Sigma\rho${C}[a]	≤0.04	0.04	0.04	0.03

[a] Cumulative fractional spin density for the carbon atoms C(1)–C(8).

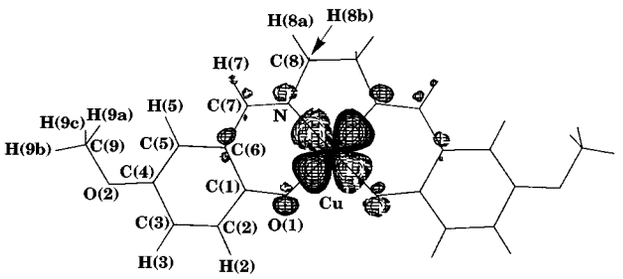

Fig. 5 Composition of the SOMO for [Cu(MeOsalen)], as calculated by the DF method. The atom numbering scheme is that employed in Table 1. The molecule has approximate C_{2v} symmetry.

SOMO of [Cu(L^1)], and those predicted by the EH, INDO/S and DF calculations, are summarised in Table 2, the SOMO derived from the DF method being displayed in Fig. 5. Only Cu, N, O(1) and H(7) (Fig. 5) contribute a fractional spin density ≥ 0.01 to the SOMO; there is an additional cumulative contribution from the carbon content of the molecule ($\Sigma\rho${C}, Table 2) that is approximately equally distributed between C(1), C(6) and C(7). Each level of theory predicts a cumulative fractional spin density of 0.90–0.91 on the [CuN$_2$O$_2$] core of the molecule, compared to the experimental value of 0.83–0.97, depending on the true value of ρ{O}. However, the EH and INDO/S calculations predict a reduced metal contribution to this orbital, and correspondingly increased contributions from the N- and O-donors, compared to the DF results. Given the approximations in our EPR calculations, there is reasonable agreement between the experimental and DF fractional spin densities.[39]

Electrochemical studies §

Cyclic voltammograms of the ligands and complexes were run in dmf–0.1 M NBu$^n_4$PF$_6$ at 293 K; the results thus obtained are summarised in Table 3. Unless otherwise stated, all potentials quoted refer to measurements run at a scan rate ('v') of 100 mV s^{-1}, and are quoted against an internal ferrocene–ferrocenium standard. Under these conditions, 2,5-dhb exhibits a single irreversible oxidation (P1) at E_{p_a} = +0.90 V with a single broad irreversible daughter (P2) at E_{p_c} = −0.52 V. Addition of up to 5 molar equivalents of 2,6-dimethylpyridine to the sample causes a broadening and a 220 mV cathodic shift of P1, reflecting deprotonation of 2,5-dhb, without affecting the potential of the P2 process. By comparison with the known voltammetric behaviour of hydroquinones in non-aqueous solvents,[40,41] we assign P1 and P2 to the processes in Scheme 2. The non-appearance of a reversible Q–Q^{2-} couple upon addition of base[41] suggests that the QH$^+$ species has an unusually high pK_a, which may reflect intramolecular hydrogen bonding to the carbaldehyde substituent (Scheme 2).[42]

The cyclic voltammograms of H$_2$L^1–H$_2$L^3 exhibit, in addition to P1 and P2, an additional irreversible daughter reduction P3

§ The nomenclature for describing the different redox states of quinones is described in ref. 39.

Table 3 Cyclic voltammetric data for the ligands and complexes (dmf–0.1 M $NBu^n_4PF_6$, 298 K, $v = 100$ mV s^{-1}). All potentials quoted *vs.* the ferrocene–ferrocenium couple. For the complexes, metal-centered processes are not listed, but are discussed in the text

	P1/P1′ E_{p_a}/V	P2/P2′ E_{p_c}/V	P3/P3′ E_{p_c}/V	P4/P4′ E_{p_a}/V	Other daughters E_{p_c}/V
2,5-dhb	+0.90	−0.52	—	—	—
H_2L^1	+0.37	−0.76	−1.24	−0.83	—
H_2L^2	+0.4[a]	−0.68	−1.15	−0.86	—
H_2L^3	+0.43	−0.59	−1.00	−0.84	—
HL^4	+0.51	−0.63	−1.41	—	—
$[Cu(L^1)]$	+0.16	−0.23	−0.96	−0.77	−0.7[a]
$[Cu(L^2)]$	+0.18	−0.28	−0.97	−0.79	−0.7[a]
$[Cu(L^3)]$	+0.28	−0.25[b]	−0.93	−0.70	−0.7,[a] −1.3[a]

[a] Broad shoulder. [b] $v = 500$ mV s^{-1}. Not detected at $v = 100$ mV s^{-1}.

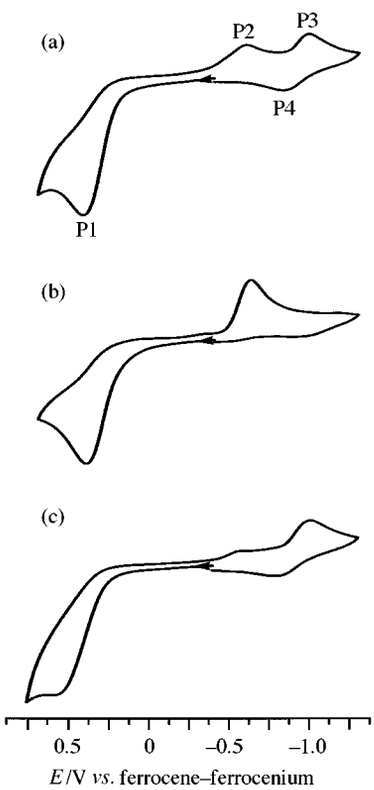

Fig. 6 Cyclic voltammograms (dmf–0.1 M $Bu^n_4NPF_6$, 298 K, 100 mV s^{-1}) of: (a) H_2L^3·MeOH; (b) H_2L^3·MeOH + 3 mole equivalents of 2,6-dimethylpyridine; (c) H_2L^3·MeOH + 5 mole equivalents of water.

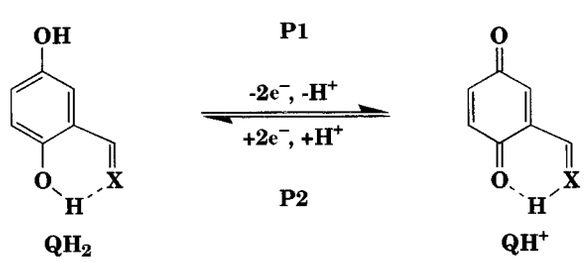

Scheme 2 X = O or NR.

with an associated reoxidation P4 [Fig. 6(a)]. At increased scan rates P2 becomes more intense relative to P3 and P4, and *vice versa*. Upon addition of 3 equivalents of 2,6-dimethylpyridine to all the ligands, P3 and P4 are no longer observed while P2 is enhanced in intensity [Fig. 6(b)]; the potential of P1 is essentially unaffected. Conversely, addition of up to 5 equivalents of MeOH or water to H_2L^1 or H_2L^2 results in diminution of P2 relative to P3/P4; the CV of H_2L^3 is similarly affected by water [Fig. (6c)], but is unchanged upon treatment with MeOH. Under conditions where P2 is not observed, the ratio of $I_{p_a}\{P1\}$: $I_{p_c}\{P3\}$ is 3.5–4.0 : 1. The cyclic voltammogram of HL^4 is

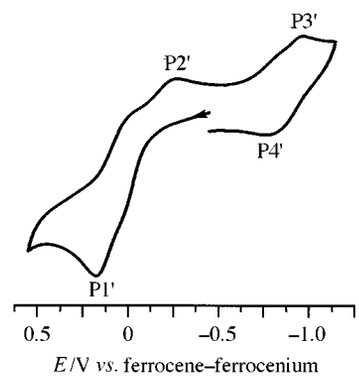

Fig. 7 Cyclic voltammogram of $[Cu(L^2)]$, showing the ligand-centered processes only (dmf–0.1 M $Bu^n_4NPF_6$, 298 K, 100 mV s^{-1}).

similar to those of the bis-imines, although a wave corresponding to P4 was not detected under any of the above conditions.

The disappearance of P3 and P4 upon addition of base [Fig. 6(b)] rules out their potential assignment as a 1,4-benzoquinone carbaldimine $Q–Q^{2-}$ couple.[41] Given the ≈4 : 1 ratio for $I_{p_a}\{P1\} : I_{p_c}\{P3\}$, P3 and P4 probably correspond to the products of a proton-catalysed ECE (electrochemical step–chemical step–electrochemical step) reaction, which will be induced by the liberation of protons at the anode following oxidation (Scheme 2). Precedent suggests three plausible pathways for the chemical step in this process: radical coupling or atom abstraction by $QH^{\bullet}$ or $QH_2^{\bullet+}$;[40] hydrolysis of the QH^+ imine moiety by adventitious moisture, followed by Michael addition of liberated amine to the quinone ring;[43] or nucleophilic attack of H_2O or, where present, MeOH at QH^+ or QH^{2+}.[44]¶ We are presently unable to distinguish between these possibilities, however, and the origin of the instability of the 1,4-benzoquinone carbaldimine function, compared to 1,4-benzoquinone carbaldehyde, is unclear.

The three copper(II) complexes show similar ligand-based redox chemistry to that of the "free" ligands, exhibiting one ligand-based oxidation (P1′) and three principal daughter peaks P2′–P4′; one or more weaker daughter reductions close to P3′ are also evident, however (Fig. 7). The P1′ oxidation shows pronounced asymmetry, which at $v \leq 25$ mV s^{-1} resolves itself into a low-potential shoulder occurring at approximately 0.5 of the total I_{p_a} for this process. The behaviour of P2′–P4′ upon varying v is identical to P2–P4 for the uncomplexed ligands. However, addition of 2,6-dimethylpyridine or MeOH to the samples did not change the relative intensities of P2′–P4′. Decomposition of 1,4-benzoquinone carbaldimines hence appears to be promoted by co-ordination to a metal ion, although it is unclear whether the P3/P4 and P3′/P4′ species result from the same ECE reaction.

¶ The presence of moderate hydrogen bond donors or acceptors such as MeOH or water has a negligible effect on the oxidation potentials of hydroquinones.[45]

The instability of our complexed ligands to electrooxidation contrasts with other voltammetric studies of σ-hydroquinonate complexes, for which chemically reversible ligand redox cycles have been reported.[4,12] Our results also contrast with the only other electrochemical study of a hydroquinone-containing Schiff base, namely that of Feringa and co-workers,[5] who prepared a dicopper complex of a bicompartmental ligand with a 2,6-di(formaldimino)-4-hydroxyphenoxy bridging group. In this case no ligand oxidation was detected within the window of the MeCN solvent, which they attributed to the presence of 2 electron-withdrawing carbaldimine substituents on the hydroquinonyl group. A more detailed study of H_2L^1–H_2L^3, their substituted derivatives and complexes with other transition ions, designed to identify the final products of ligand oxidation, is in progress and will be reported separately.

In addition to the ligand-centred processes, [Cu(L^1)]–[Cu(L^3)] exhibit a reduction with $I_{p_c} = (0.2–0.3)I_{p_a}\{P1'\}$, which we assign as a Cu^{II}–Cu^{I} reduction. For [Cu(L^1)] and [Cu(L^2)] this process is irreversible, occurring at $E_{p_c} = -1.9$ V; for [Cu(L^3)] a reversible Cu^{II}–Cu^{I} couple at $E_{\frac{1}{2}} = -1.70$ V is observed. Compound [Cu(L^3)] also exhibits an irreversible peak at $E_{p_c} = -2.56$ V with no detectable daughters, which we attribute to a ligand reduction associated with the $[L^3]^{2-}$ phenylenediimine moiety.

Experimental

Unless stated otherwise, all manipulations were performed in air using commercial grade solvents. Electrochemical studies employed anhydrous 99.8% dmf (Aldrich). 2,5-Dihydroxybenzaldehyde, methylamine (1.0 M solution in MeOH), *trans*-1,2-diaminocyclohexane (Aldrich), 1,2-phenylenediamine, 1,2-ethylenediamine and $Cu(O_2CMe)_2{\cdot}H_2O$ (Avocado) were used as supplied; H_2L^1 was prepared by the literature method.[7]

Syntheses

***N*,*N*′-Bis(2,5-dihydroxybenzylidene)-*trans*-1,2-diaminocyclohexane (H_2L^2).** 2,5-Dihydroxybenzaldehyde (2.0 g, 1.45×10^{-2} mol) and *trans*-1,2-diaminocyclohexane (0.83 g, 7.25×10^{-3} mol) were refluxed in MeOH (50 cm^3) for 3 h, affording a bright yellow solution which was evaporated to a yellow oil. Trituration of this oil with Et_2O yielded a mustard yellow microcrystalline solid, which was filtered off, washed with Et_2O and dried *in vacuo*. Yield 2.2 g, 86% (Found: C, 67.7; H, 6.3; N, 7.9. Calc. for $C_{10}H_{11}NO_2$: C, 67.8; H, 6.3; N, 7.8%), mp 195 °C (decomp.). FAB mass spectrum: *m*/*z* 355 $[M + H]^+$; and 354, $[M]^+$. ^{1}H NMR [$(CD_3)_2SO$]: δ 12.47 [s, 2 H, phenyl OH^2], 8.96 [s, 2 H, OH^5], 8.36 [s, 2 H, CH=N], 6.72 [dd, $J = 2.8$, 9.1, 2 H, phenyl H^4], 6.72 [d, $J = 2.8$, 2 H, phenyl H^6], 6.64 [d, $J = 9.1$ Hz, 2 H, phenyl H^3], 3.33 [m, 2 H, cyclohexyl CHN] and 1.42–1.86 [m, 8 H, cyclohexyl CH_2].

***N*,*N*′-Bis(2,5-dihydroxybenzylidene)-1,2-diaminobenzene (H_2L^3).** 2,5-Dihydroxybenzaldehyde (2.0 g, 1.45×10^{-2} mol) and 1,2-phenylenediamine (0.78 g, 7.25×10^{-3} mol) were refluxed in MeOH (50 cm^3) for 3 h. The resultant brick red precipitate was filtered off, washed with MeOH until the washings were colourless, washed with Et_2O and dried *in vacuo*. Yield 1.8 g, 72% (Found: C, 66.4; H, 5.3; N, 7.5. Calc. for $C_{20}H_{16}NO_4{\cdot}CH_3OH$: C, 66.3; H, 5.3; N, 7.4%), mp 140 °C (decomp.). FAB mass spectrum: *m*/*z* 349, $[M + H]^+$; and 348, $[M]^+$. ^{1}H NMR [$(CD_3)_2SO$]: δ 12.18 [s, 2 H, phenyl OH^2], 9.14 [s, 2 H, phenyl OH^5], 8.82 [s, 2 H, CH=N], 7.41 [m, 4 H, phenylene CH], 7.06 [d, $J = 2.9$, 2 H, phenyl H^6], 6.89 [dd, $J = 2.9$, 8.8, 2 H, phenyl H^4], 6.81 [d, $J = 8.8$, 2 H, phenyl H^3], 4.13 [q, $J = 5.3$, 1 H, $CH_3O\mathit{H}$] and 3.17 [d, $J = 5.3$ Hz, 3 H, $C\mathit{H}_3OH$].

2,5-Dihydroxybenzylidenemethylamine (HL^4). 2,5-Dihydroxybenzaldehyde (0.5 g, 3.63×10^{-3} mol) and methylamine (3.63 cm^3 of a 1.0 M solution in MeOH, 3.63×10^{-3} mol) were stirred in MeOH (20 cm^3) for 1 h. The resultant orange solution was evaporated to an orange microcrystalline residue, which was washed with the minimum volume of Et_2O and dried *in vacuo*. Yield 0.48 g, 88% (Found: C, 63.3; H, 6.0; N, 9.0. Calc. for $C_8H_9NO_2$: C, 63.6; H, 6.0; N, 9.3%), mp 105 °C (decomp.). FAB mass spectrum: *m*/*z* 152, $[M + H]^+$; 151, $[M]^+$. ^{1}H NMR [$(CD_3)_2SO$]: δ 12.55 [s, 1 H, phenyl OH^2], 8.93 [s, 1 H, OH^5], 8.44 [s, 1 H, CH=N], 6.79 [d, $J = 2.9$, 1 H, phenyl H^6], 6.72 [dd, $J = 2.9$, 8.7, 1 H, phenyl H^4], 6.58 [d, $J = 8.7$ Hz, 1 H, phenyl H^3] and 3.41 [s, 3 H, CH_3].

[*N*,*N*′-Bis(2,5-dihydroxybenzylidene)-1,2-diaminoethanato]copper(II) ([Cu(L^1)]). A MeOH solution of 2,5-dihydroxybenzaldehyde (0.20 g, 1.45×10^{-3} mol), 1,2-ethylenediamine (0.044 g, 7.25×10^{-4} mol) and $Cu(O_2CMe)_2{\cdot}H_2O$ (0.14 g, 7.25×10^{-4} mol) was refluxed for 2 h, to give a brown precipitate. This was filtered off, washed with MeOH until the washings were colourless, washed with Et_2O and dried *in vacuo*. Yield 0.17 g, 66% (Found: C, 50.0; H, 4.2; N, 7.2. Calc. for $C_{16}H_{14}CuN_2O_4{\cdot}H_2O$: C, 50.0; H, 4.2; N, 7.4%). FAB mass spectrum: *m*/*z* 362, $[^{63}Cu(L^1) + H]^+$; and 361, $[^{63}Cu(L^1)]^+$. UV/vis spectrum (dmf): ν_{max} 17500 ($\varepsilon_{max} = 420$), 24800 (9800 M^{-1} cm^{-1}), and 36600 (sh) cm^{-1}.

[*N*,*N*′-Bis(2,5-dihydroxybenzylidene)-1,2-diaminocyclohexanato]copper(II) ([Cu(L^2)]). *Method A.* As for [Cu(L^1)], employing *trans*-1,2-diaminocyclohexane (0.083 g, 7.25×10^{-4} mol). Yield 0.22 g, 73% (Found: C, 56.0; H, 5.3; N, 6.3. Calc. for $C_{20}H_{20}CuN_2O_4{\cdot}CH_3OH$: C, 56.3; H, 5.4; N, 6.2%). FAB mass spectrum: *m*/*z* 416, $[^{63}Cu(L^2) + H]^+$; and 415, $[^{63}Cu(L^2)]^+$. UV/vis spectrum (dmf): ν_{max} 17700 ($\varepsilon_{max} = 410$), 24800 (10500 M^{-1} cm^{-1}) and 36000 (sh) cm^{-1}.

Method B. Solutions of H_2L^2 (0.50 g, 1.41×10^{-3} mol) and $Cu(O_2CMe)_2{\cdot}H_2O$ (0.28 g, 1.41×10^{-3} mol) were mixed at room temperature and allowed to stand for 1 h. The resultant deep brown microcrystals were filtered off, washed with MeCN and EtO, and dried *in vacuo*. Yield 0.48 g, 82% (Found: C, 56.6; H, 5.0; N, 8.0. Calc. for $C_{20}H_{20}CuN_2O_4{\cdot}0.5H_2O{\cdot}0.5CH_3CN$: C, 56.6; H, 5.1; N, 7.9%).

[*N*,*N*′-Bis(2,5-dihydroxybenzylidene)-1,2-diaminobenzenato]copper(II) ([Cu(L^3)]). *Method A.* As for [Cu(L^1)], employing 1,2-diaminobenzene (0.078 g, 7.25×10^{-4} mol). Yield 0.23 g, 78% (Found: C, 56.6; H, 4.2; N, 6.4. Calc. for $C_{20}H_{14}CuN_2O_4{\cdot}CH_3OH$: C, 57.0; H, 4.1; N, 6.3%). FAB mass spectrum: *m*/*z* 410, $[^{63}Cu(L^3) + H]^+$; 409, $[^{63}Cu(L^3)]^+$. UV/vis spectrum (dmf): ν_{max} 15400 (sh), 21200 ($\varepsilon_{max} = 16500$), 24200 (sh), 28400 (sh), 29900 (19800), 31800 (22700 M^{-1} cm^{-1}), 32500 (sh) and 36600 (sh) cm^{-1}.

Method B. As for [Cu(L^2)], using $H_2L^3{\cdot}CH_3OH$ (0.53 g, 1.41×10^{-3} mol). Yield 0.48 g, 82% (Found: C, 57.3; H, 3.7; N, 7.8. Calc. for $C_{20}H_{14}CuN_2O_4{\cdot}0.5H_2O{\cdot}0.5CH_3CN$: C, 57.4; H, 3.8; N, 8.0%).

Other measurements

Infrared spectra were obtained as Nujol mulls pressed between KBr windows at 400–4000 cm^{-1} using a Perkin-Elmer Paragon 1000 spectrophotometer, UV/visible spectra with a Perkin-Elmer Lambda 12 spectrophotometer operating between 1100 and 200 nm in 1 cm quartz cells, positive ion fast atom bombardment mass spectra on a Kratos MS890 spectrometer, employing a 3-nitrobenzyl alcohol matrix, and NMR spectra on a Bruker DPX250 spectrometer, operating at 250.1 MHz (^{1}H). The CHN microanalyses were performed by the University of Cambridge Department of Chemistry microanalytical service. Melting points are uncorrected. The EPR spectra were obtained using a Bruker ESP300E spectrometer; X-band spectra employed an ER4102ST resonator and ER4111VT

cryostat, while for Q-band spectra an ER5106QT resonator and an ER4118VT cryostat were used. Spectral simulations were performed using in-house software which has been described elsewhere.[44] ENDOR Spectra were recorded on a Bruker ESP300E X-band EPR spectrometer fitted with an ESP360 DICE ENDOR unit coupled to an EIN A-300 RF power amplifier operating between 300 and 500 W (8 dB). A Bruker EN 801 ENDOR cavity fitted with an Oxford Instruments ESR 900 liquid helium cryostat was used for the experiments, employing a modulation frequency of 12.5 kHz.

Electrochemical measurements were carried out using an Autolab PGSTAT20 voltammetric analyser, in dmf containing 0.1 M $NBu^n_4PF_6$ (prepared from aqueous NBu^n_4OH and HPF_6, recrystallised twice from MeOH) as supporting electrolyte. Cyclic voltammetric experiments employed a double platinum working/counter electrode and a silver wire reference electrode; all potentials are referenced to an internal ferrocene–ferrocenium standard and were obtained at a scan rate of 100 mV s^{-1}.

EHMO Calculations were carried out using the CACAO package,[46] while INDO/S calculations were performed using the Argus package written by Thompson.[47] Density functional calculations were performed using the DEFT code written by St-Amant[48] in the linear combination of Gaussian-type orbitals framework. The calculations used the Vosko–Wilk–Nusair[49] local spin density approximation of the correlation part of the exchange-correlation potential with the Becke[50] non-local functional for exchange and the Perdew[51] non-local functional for correlation. The all-electron treatment used Gaussian basis functions of double-zeta quality with contraction patterns (721/51/1*) for carbon, nitrogen and oxygen, (63321/531*/41+) for copper and (41/1*) for hydrogen. All calculations employed the crystal structure coordinates for [Cu(MeOsalen)][24] oriented with the global z axis lying perpendicular to the approximately planar CuO_2N_2 unit and the x axis bisecting the co-ordinated oxygen atoms. The symmetry of the first co-ordination sphere of the copper ion is approximately C_{2v}.

Acknowledgements

The authors thank the Royal Society (London) for a University Research Fellowship to M. A. H., the Government of Singapore (L. M. L. C.), the EPSRC and the University of Cambridge for financial support. The authors would like to thank Dr D. M. Murphy (EPSRC ENDOR centre) for useful discussions, and Dr A. St-Amant (University of Ottawa) for making the DEFT software publically available.

References

1 C. G. Pierpont and R. M. Buchanan, *Coord. Chem. Rev.*, 1981, **38**, 45; C. G. Pierpont and C. W. Lange, *Prog. Inorg. Chem.*, 1994, **41**, 331.
2 C. Floriani, G. Fachinetti and F. Calderazzo, *J. Chem. Soc.*, *Dalton Trans.*, 1973, 765; L. Kessel and D. N. Hendrickson, *Inorg. Chem.*, 1978, **17**, 2630; R. H. Heistand II, A. L. Roe and L. Que, Jr., *Inorg. Chem.*, 1982, **21**, 676.
3 M. Handa, H. Sono, K. Kasamatsu, K. Kasuga, M. Mikuriya and S. Ikenoue, *Chem. Lett.*, 1992, 453; M. Handa, A. Takata, T. Nakao, K. Kasuga, M. Mikuriya and T. Kotera, *Chem. Lett.*, 1992, 2085; M. Handa, H. Matsumoto, T. Namura, T. Nagaoka, K. Kasuga, M. Mikuriya, T. Kotera and R. Nukada, *Chem. Lett.*, 1995, 903; M. Handa, M. Mikuriya, Y. Sato, T. Kotera, R. Nukada, D. Yoshioka and K. Kasuga, *Bull. Chem. Soc. Jpn.*, 1996, **69**, 3483; M. Handa, T. Nakao, M. Mikuriya, T. Kotera, R. Nukada and K. Kasuga, *Inorg. Chem.*, 1998, **37**, 149.
4 S. Ernst, P. Hänel, J. Jordanov, W. Kaim, V. Kasack and E. Roth, *J. Am. Chem. Soc.*, 1989, **111**, 1733.
5 O. J. Gelling, A. Meetsma and B. L. Feringa, *Inorg. Chem.*, 1990, **29**, 2816.
6 G. Asgedom, A. Sreedhara, E. Kolehmainen and C. P. Rao, *J. Chem. Soc.*, *Dalton Trans.*, 1996, 93.
7 M. Calvin and C. H. Barkelew, *J. Am. Chem. Soc.*, 1946, **68**, 2267; T. Tanaka, *Bull. Chem. Soc. Jpn.*, 1960, 259; T. D. Shaffer and K. A. Sheth, *Mol. Cryst. Liq. Cryst.*, 1989, **172**, 27; S. E. Byström, E. M. Larsson and B. Åkermark, *J. Org. Chem.*, 1990, **55**, 5674.
8 R. A. Berthon, S. B. Colbran and D. C. Craig, *Polyhedron*, 1992, **11**, 243; R. A. Berthon, S. B. Colbran and G. M. Moran, *Inorg. Chim. Acta*, 1993, **204**, 3; S. B. Sembiring, S. B. Colbran and D. C. Craig, *Inorg. Chem.*, 1995, **34**, 761; S. B. Sembiring, S. B. Colbran, R. Bishop, D. C. Craig and A. D. Rae, *Inorg. Chim. Acta*, 1995, **228**, 109; S. B. Sembiring, S. B. Colbran, D. C. Craig and M. L. Scudder, *J. Chem. Soc.*, *Dalton Trans.*, 1995, 3731.
9 C. D. Stevenson, R. C. Reiter, R. D. Burton and T. D. Halvorsen, *Inorg. Chem.*, 1995, **34**, 1368.
10 J. Li, V. Katti, A. A. Pinkerton, H. Nar and R. G. Cavell, *Can. J. Chem.*, 1996, **74**, 2378.
11 P. Cornago, C. Escolástico, M. D. Santa María, R. M. Claramunt, D. Carmona, M. Esteban, L. A. Oro, C. Foces-Foces, A. L. Llamas-Saiz and J. Elguero, *J. Organomet. Chem.*, 1994, **467**, 293.
12 T. E. Keyes, P. M. Jayaweera, J. J. McGarvey and J. G. Vos, *J. Chem. Soc.*, *Dalton Trans.*, 1997, 1627.
13 R. H. Bailes and M. Calvin, *J. Am. Chem. Soc.*, 1947, **69**, 1886.
14 R. S. Downing and F. L. Urbach, *J. Am. Chem. Soc.*, 1969, **91**, 5977.
15 T. N. Waters and D. Hall, *J. Chem. Soc.*, 1959, 1200.
16 R. Atkins, G. Brewer, E. Kokot, G. M. Mockler and E. Sinn, *Inorg. Chem.*, 1985, **24**, 127.
17 D. F. Rohrbach, W. R. Heineman and E. Deutsch, *Inorg. Chem.*, 1979, **18**, 2536.
18 K. Bernardo, S. Leppard, A. Robert, G. Commenges, F. Dahan and B. Meunier, *Inorg. Chem.*, 1996, **35**, 387.
19 T. Tanaka, K. Tsurutani, A. Komatsu, T. Ito, K. Iida, Y. Fujii, Y. Nakano, Y. Usui, Y. Fukuda and M. Chikira, *Bull. Chem. Soc. Jpn.*, 1997, **70**, 615.
20 B. Bosnich, *J. Am. Chem. Soc.*, 1968, **90**, 627; A. C. Braithwaite, P. E. Wright and T. N. Waters, *J. Inorg. Nucl. Chem.*, 1975, **37**, 1669.
21 E. Suresh, M. M. Bhadbhade and D. Srinivas, *Polyhedron*, 1996, **15**, 4133.
22 G. M. Larin, V. M. Dziomko, K. A. Dunaevskaya and Y. K. Syrkin, *Zh. Strukt. Khim.*, 1965, **6**, 391; G. M. Larin, G. V. Panova and E. G. Rukhadze, *Zh. Strukt. Khim.*, 1965, **6**, 699; *Dokl. Akad. Nauk SSSR*, 1966, **166**, 363.
23 E. Hasty, T. J. Colburn and D. N. Hendrickson, *Inorg. Chem.*, 1973, **12**, 2414.
24 M. M. Bhadbhade and D. Srinivas, *Inorg. Chem.*, 1993, **32**, 6122.
25 T. Lund and W. E. Hatfield, *J. Chem. Phys.*, 1973, **59**, 885; A. D. Toy, M. D. Hobday, P. D. W. Boyd and T. D. Smith, *J. Chem. Soc.*, *Dalton Trans.*, 1973, 1259; M. Chikira, H. Yokoi and T. Isobe, *Bull. Chem. Soc. Jpn.*, 1974, **47**, 2208.
26 A. H. Maki and B. R. McGarvey, *J. Chem. Phys.*, 1958, **29**, 31, 35.
27 B. A. Goodman and J. B. Raynor, *Adv. Inorg. Chem.*, 1970, **13**, 135.
28 B. M. Hoffman, J. Martinsen and R. A. Venters, *J. Magn. Reson.*, 1984, **59**, 110.
29 D. Kivelson and R. Neiman, *J. Chem. Phys.*, 1961, **35**, 149.
30 V. G. Swett and E. P. Dudek, *J. Phys. Chem.*, 1968, **72**, 1244; I. Adato, A. H. I. Ben-Bassat and S. Sarel, *J. Phys. Chem.*, 1971, **75**, 3828.
31 A. Abragam and M. H. L. Pryce, *Proc. R. Soc. London*, *Ser. A*, 1951, **206**, 164.
32 J. Ferguson, *J. Chem. Phys.*, 1961, **34**, 2206; R. L. Belford and T. Piper, *Mol. Phys.*, 1962, **5**, 251.
33 C. D. Olson, G. Basu and R. L. Belford, *J. Coord. Chem.*, 1971, **1**, 176.
34 M. A. Hitchman, *Inorg. Chem.*, 1977, **16**, 1985.
35 A. G. Prudell and P. Kusch, *Phys. Rev.*, 1952, **88**, 184.
36 A. J. Bridgeman and M. Gerloch, *Prog. Inorg. Chem.*, 1996, **45**, 179.
37 M. J. Duer, N. D. Fenton and M. Gerloch, *Int. Rev. Phys. Chem.*, 1990, **9**, 227.
38 J. E. Huyett, S. B. Choudhury, D. M. Eichhorn, P. A. Bryngelson, M. J. Maroney and B. M. Hoffman, *Inorg. Chem.*, 1998, **37**, 1361.
39 J. Q. Chambers, *The Chemistry of the Quinoid Compounds*, ed. S. Patai, Wiley, New York, 1974, ch. 14, pp. 737–791; J. Q. Chambers, *The Chemistry of the Quinoid Compounds*, *vol. 2*, eds. S. Patai and Z. Rappoport, Wiley, New York, 1988, ch. 12, pp. 719–757.
40 B. R. Eggins and J. Q. Chambers, *Chem. Commun.*, 1969, 232; V. D. Parker, *Chem. Commun.*, 1969, 716; B. R. Eggins and J. Q. Chambers, *J. Electrochem. Soc.*, 1970, **117**, 186.
41 See *e.g.* R. Wang, T. E. Keyes, R. Hage, R. H. Schmehl and J. G. Vos, *J. Chem. Soc.*, *Chem. Commun.*, 1993, 1652.
42 M. Z. Barakat, S. K. Shebab and M. M. El-Sadr, *J. Chem. Soc.*, 1958, 901; W. Schäfer and A. Aguado, *Angew. Chem.*, *Int. Ed. Engl.*, 1971, **10**, 405; G. D. Storrier, S. B. Colbran and D. C. Craig, *J. Chem. Soc.*, *Dalton Trans.*, 1997, 3011.

43 L. Papouchado, G. Petrie, J. H. Sharp and R. N. Adams, *J. Am. Chem. Soc.*, 1968, **90**, 5620.
44 F. E. Mabbs and D. Collison, *Electron Paramagnetic Resonance of d Transition Metal Compounds*, Elsevier, Amsterdam, 1992, ch. 7.
45 See *e.g.* J. A. Lanning and J. Q. Chambers, *Anal. Chem.*, 1973, **45**, 1010; N. Guptan and H. Lipschitz, *J. Am. Chem. Soc.*, 1997, **119**, 6384.
46 C. Mealli and D. M. Proserpio, *J. Chem. Educ.*, 1990, **67**, 399.
47 M. A. Thompson, Battelle Pacific Northwest Laboratories, 1992.
48 A. St-Amant, DEFT, A FORTRAN program, University of Ottawa, 1994.
49 S. H. Vosko, L. Wilk and M. Nusair, *Can. J. Phys.*, 1980, **58**, 1200.
50 A. D. Becke, *Phys. Rev. A*, 1988, **38**, 3098.
51 J. P. Perdew, *Phys. Rev. B*, 1986, **33**, 8822.

Paper 9/02294E